Electronic Supplementary Material (ESI) for Soft Matter.
This journal is © The Royal Society of Chemistry 2019

Supporting Information

Microextrusion Printing Cell-Laden Networks of Type I Collagen with Patterned Fiber Alignment and Geometry

*Bryan A. Nerger, P.-T. Brun, and Celeste M. Nelson**

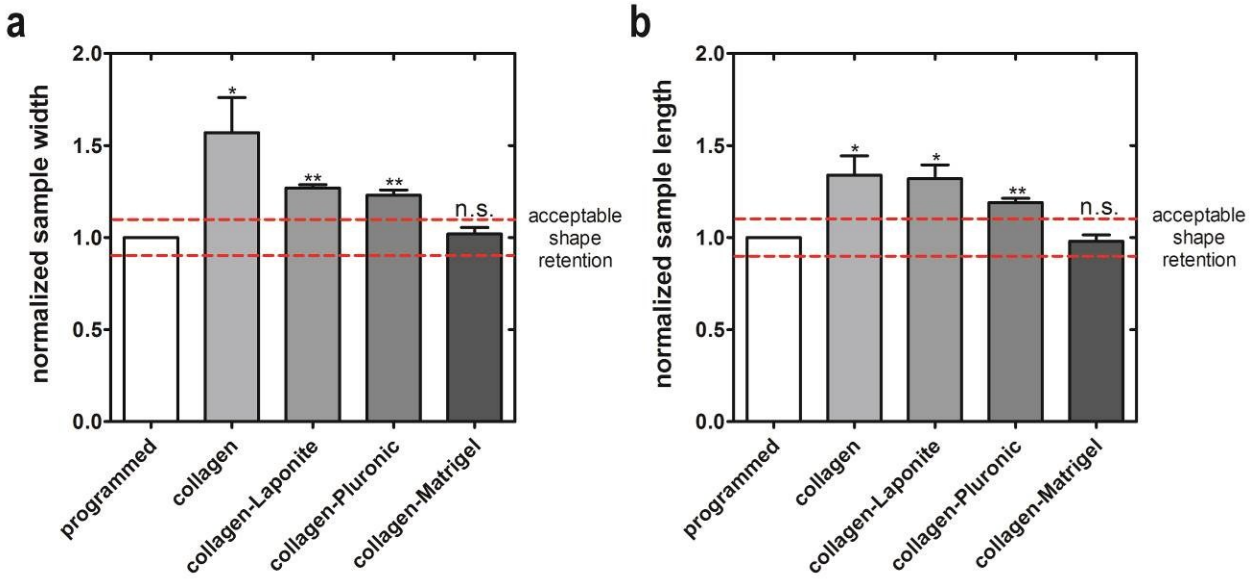

Figure S1. Shape retention of collagen inks. Normalized sample a) width and b) length of rectangular geometries that were 3D printed with collagen ink formulations. "Programmed" represents the dimensions of the printing path, while normalized dimensions are calculated by taking the ratio of measured dimensions relative to the programmed dimensions. Dashed red lines represent the criteria for acceptable shape retention (±10% of programmed dimensions). *$p \leq 0.05$; **$p \leq 0.01$; n.s., not significant.

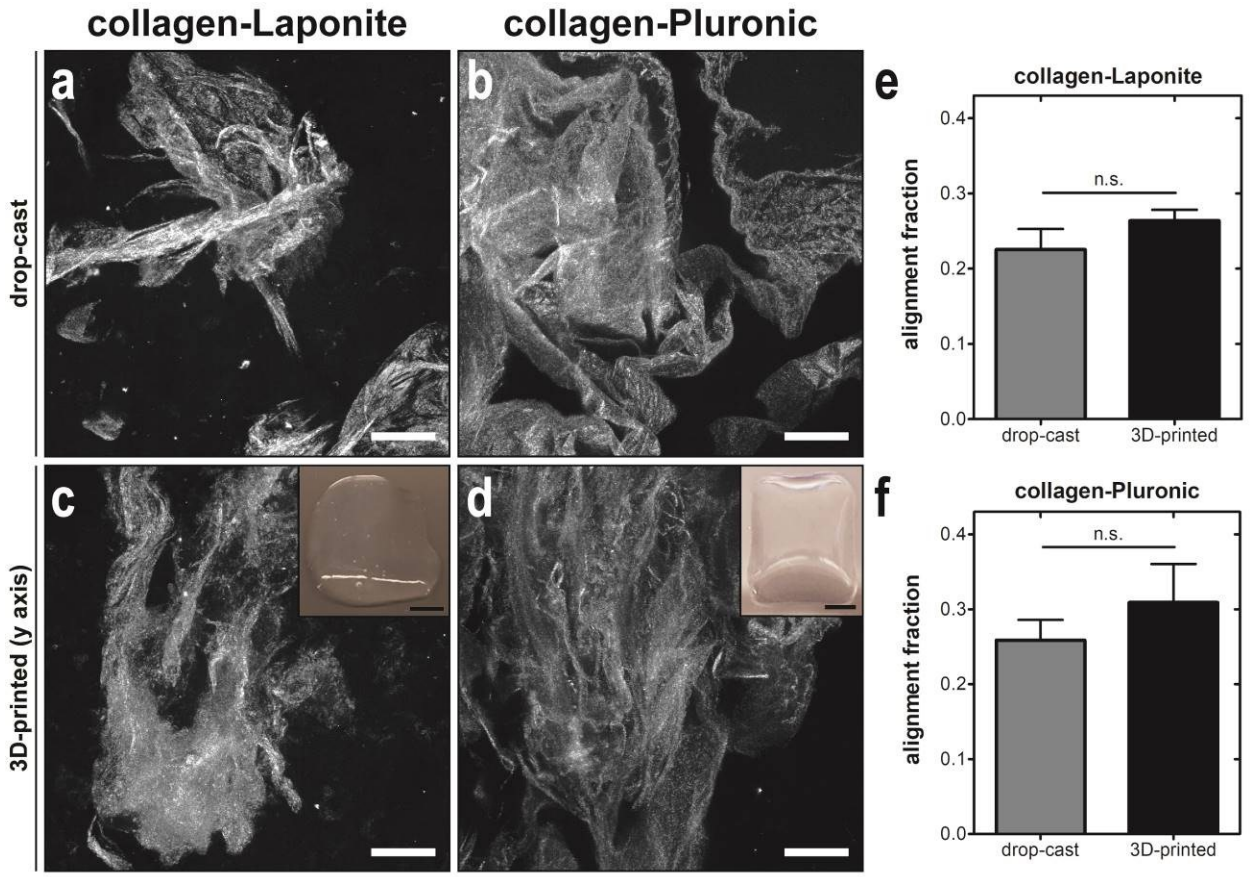

Figure S2. Morphology and alignment of collagen-Laponite and collagen-Pluronic inks. CRM images of drop-cast a) collagen-Laponite and b) collagen-Pluronic and 3D-printed c) collagen-Laponite and d) collagen-Pluronic. All CRM images represent the maximum-intensity z-projection of a single 30-µm-thick z-stack. Optical images are representative 3D-printed rectangular samples. Samples were 3D printed using a 254-µm-diameter conical nozzle at a printing speed of 40 mm/s. Scale bars on CRM images represent 50 µm, and scale bars on optical images represent 2.5 mm. Average alignment fraction of drop-cast and 3D-printed samples of e) collagen-Laponite and f) collagen-Pluronic. n.s., not significant.

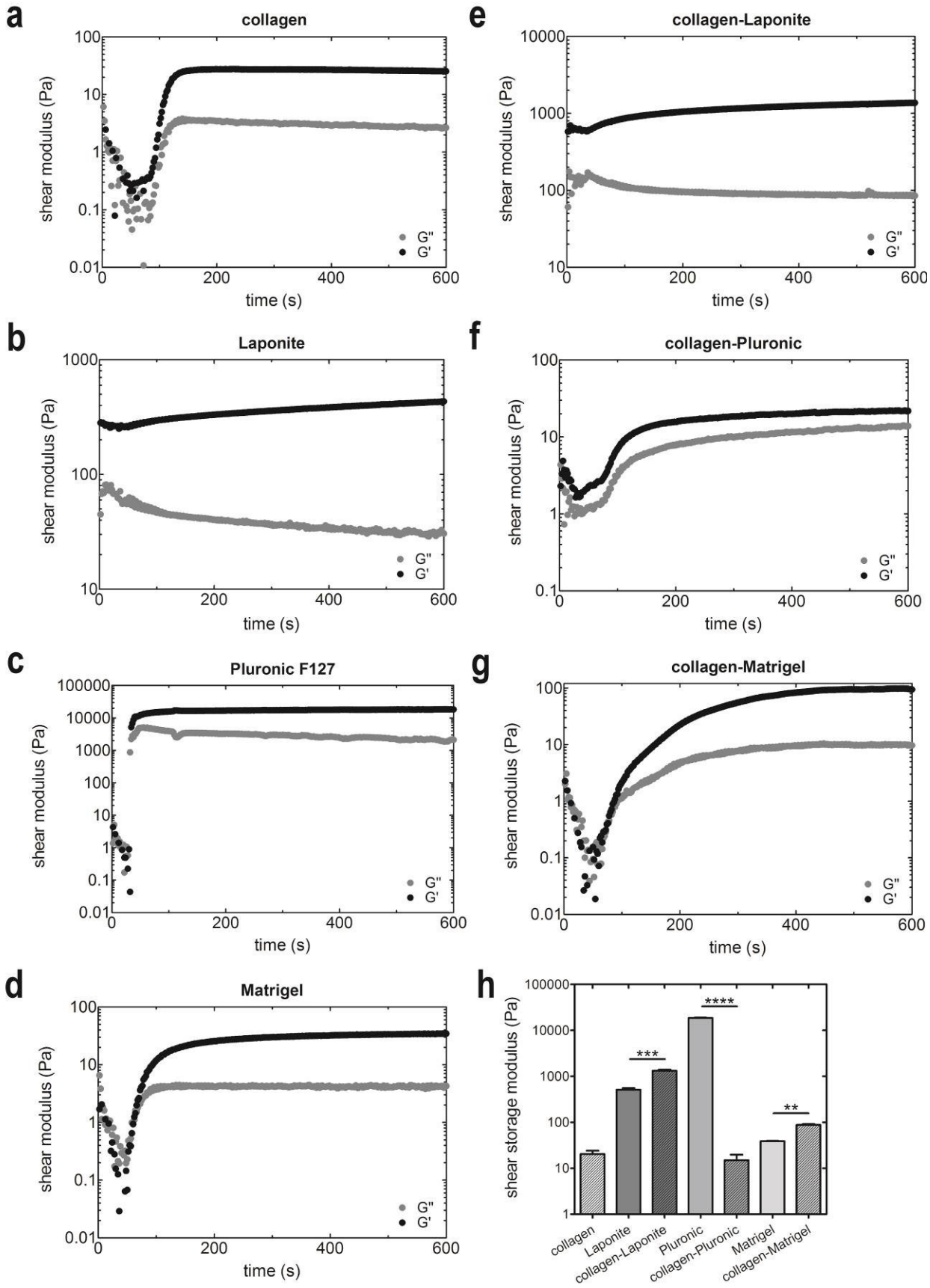
a
collagen
shear modulus (Pa)
time (s)
G''
G'
b
Laponite
c
Pluronic F127
d
Matrigel
e
collagen-Laponite
f
collagen-Pluronic
g
collagen-Matrigel
h
shear storage modulus (Pa)
***
****
**
collagen
Laponite
collagen-Laponite
Pluronic
collagen-Pluronic
Matrigel
collagen-Matrigel

Figure S3. Shear storage and loss moduli of collagen inks. Representative temperature-dependent storage and loss moduli for a) 0.8 mg/ml type I collagen, b) 3 mg/ml Laponite, c) 250 mg/ml Pluronic F127, d) 8.2 mg/ml Matrigel, e) collagen-Laponite, f) collagen-Pluronic, or g) collagen-Matrigel. Data from first replicate is plotted; outliers at early time points were excluded. h) Average steady-state storage moduli of collagen inks. Shown are mean ± standard deviation. $^{**}p \leq 0.01$; $^{***}p \leq 0.001$; $^{****}p \leq 0.0001$.

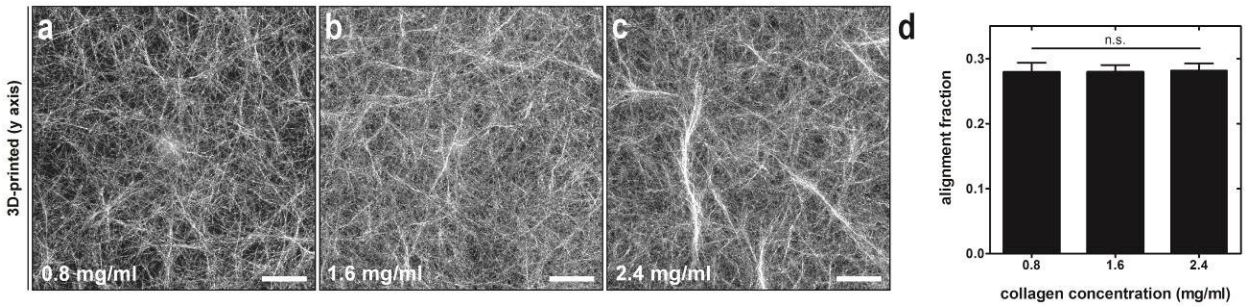

Figure S4. 3D printing different concentrations of type I collagen. CRM images of type I collagen inks with concentrations of a) 0.8 mg/ml, b) 1.6 mg/ml, or c) 2.4 mg/ml. d) Alignment fraction of 3D-printed collagen samples with different collagen concentrations. Scale bars = 50 μm. All CRM images represent the maximum-intensity z-projection of a 30-μm-thick z-stack. All samples were 3D-printed using a 254-μm-diameter nozzle at a printing speed of 40 mm/s. n.s., not significant.

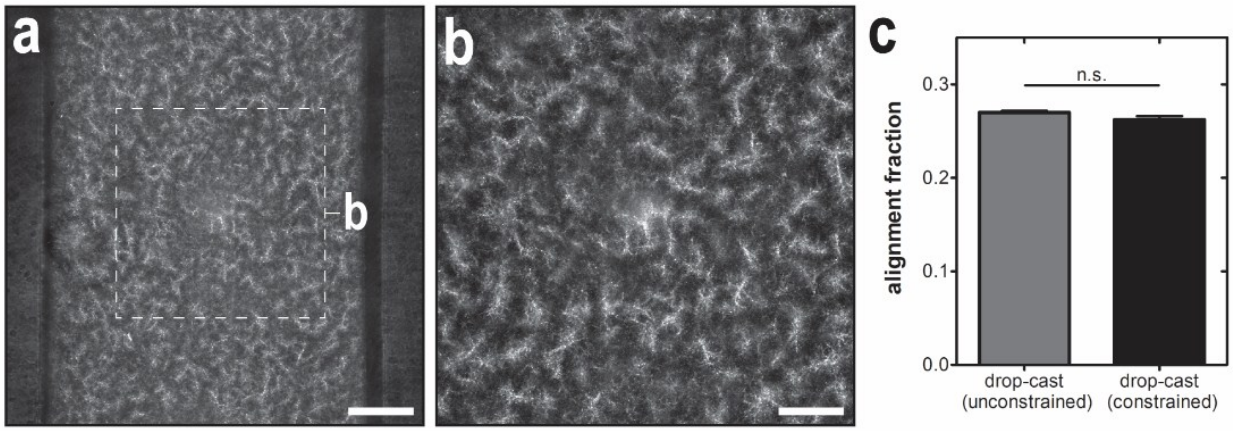

Figure S5. Collagen fiber alignment in unconstrained and constrained drop-cast collagen-Matrigel inks. a) Low-magnification (scale bar = 200 μm) and b) high-magnification (scale bar = 100 μm) CRM images of collagen-Matrigel inks drop cast into a microfluidic channel (~1 mm width and height). c) Alignment fraction of collagen-Matrigel inks drop cast onto an unpatterned substratum (unconstrained) and a microfluidic channel (constrained). All images represent the maximum-intensity z-projection of a 30-μm z-stack. Each independent replicate for the drop-cast (constrained) condition consisted of two samples. n.s., not significant.

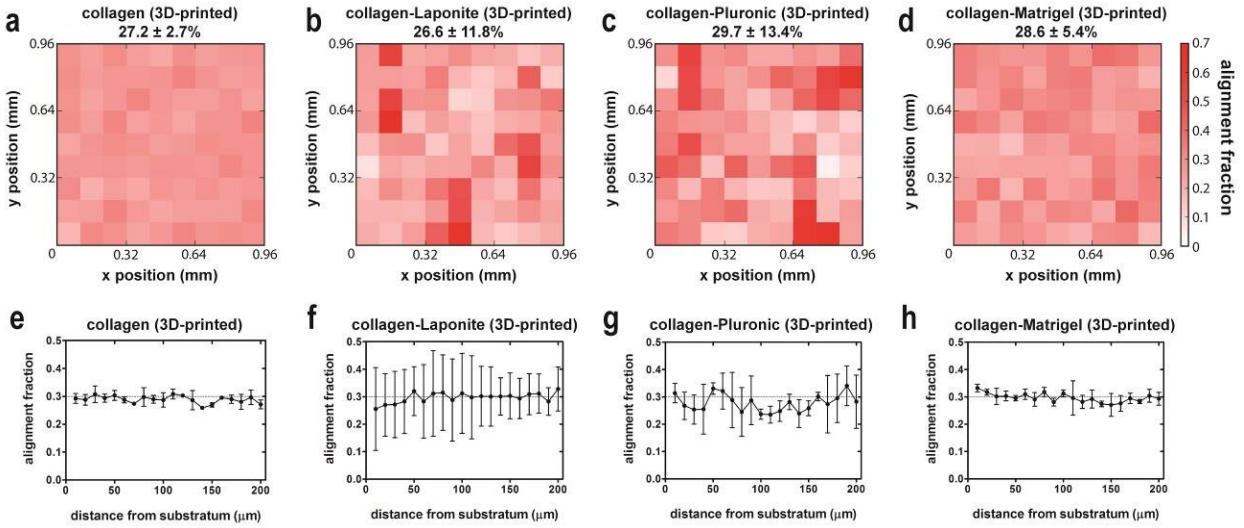

Figure S6. Quantifying collagen fiber alignment in 3D-printed rectangular samples. Alignment fraction heat map for a representative sample of 3D-printed a) type I collagen, b) collagen-Laponite, c) collagen-Pluronic, or d) collagen-Matrigel. The average alignment fraction and corresponding standard deviation are displayed above each heat map. Alignment fraction as a function of depth for a representative sample of 3D-printed e) type I collagen, f) collagen-Laponite, g) collagen-Pluronic, or h) collagen-Matrigel. The dotted reference line indicates an alignment fraction of 0.3. All samples were printed using a 254-μm-diameter nozzle at a printing speed of 40 mm/s.

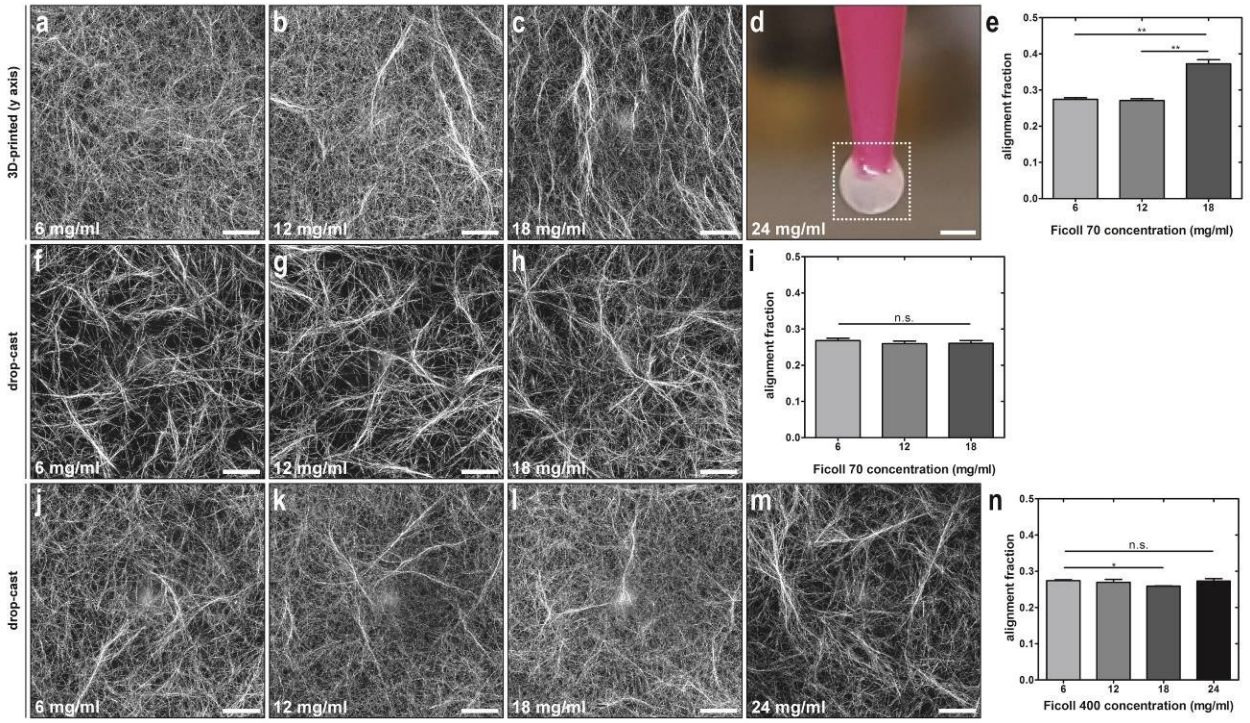

Figure S7. 3D-printed and drop-cast collagen-Ficoll inks. CRM images of 3D-printed collagen inks containing Ficoll 70 at concentrations of a) 6 mg/ml, b) 12 mg/ml, or c) 18 mg/ml. d) Optical image of the 3D-printing nozzle used to print a collagen-Ficoll 70 ink with a Ficoll 70 concentration of 24 mg/ml. The image shows polymerized collagen blocking the nozzle in the region enclosed in white dashed lines (scale bar = 1 mm). e) Alignment fraction for 3D-printed collagen-Ficoll 70 inks. CRM images of drop-cast collagen inks containing Ficoll 70 concentrations of f) 6 mg/ml, g) 12 mg/ml, or h) 18 mg/ml. i) Alignment fraction for drop-cast collagen-Ficoll 70 inks. CRM images of drop-cast collagen inks containing Ficoll 400 concentrations of j) 6 mg/ml, k) 12 mg/ml, l) 18 mg/ml, or m) 24 mg/ml. n) Alignment fraction for drop-cast collagen-Ficoll 400 inks. Scale bars = 50 μm. All CRM images represent the maximum-intensity z-projection of a 30-μm z-stack. *$p \leq 0.05$; **$p \leq 0.01$; n.s., not significant.

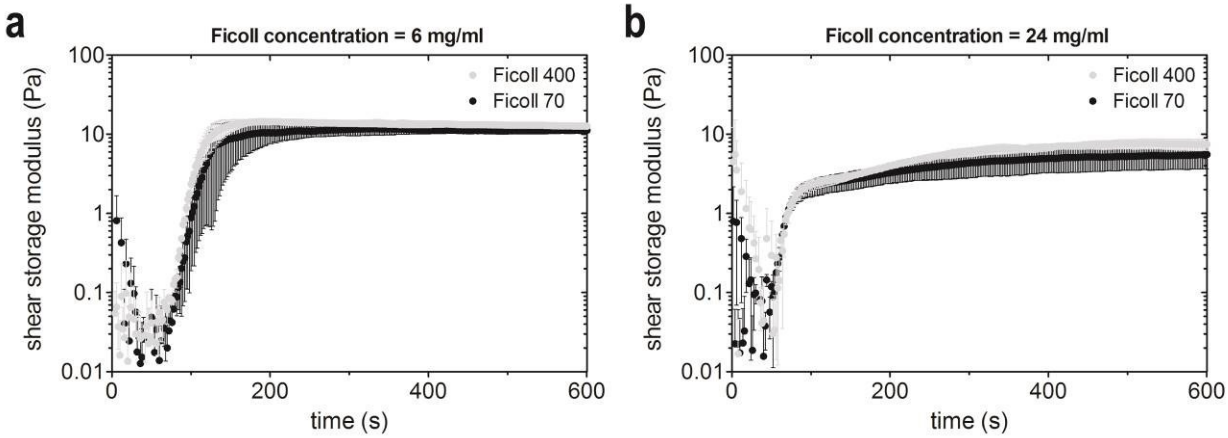

Figure S8. Shear storage moduli of collagen-Ficoll inks. Representative temperature-dependent shear storage moduli for collagen-Ficoll 70 and collagen-Ficoll 400 inks containing Ficoll concentrations of a) 6 mg/ml and b) 24 mg/ml. Shown are mean ± standard deviation.

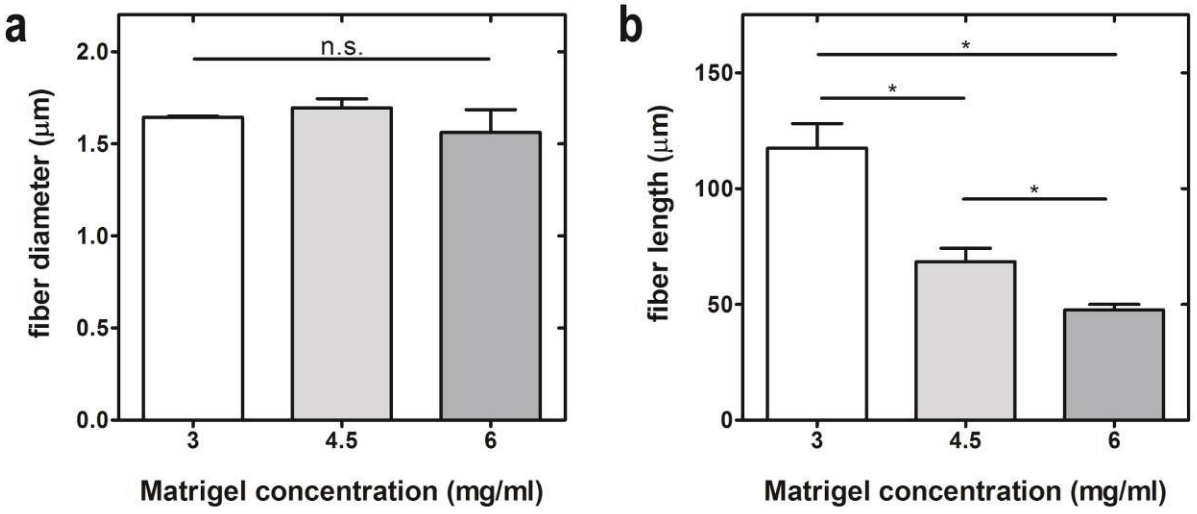

Figure S9. Collagen fiber diameter and length as a function of Matrigel protein concentration. Average a) collagen fiber diameter and b) length of collagen fiber bundles in 3D-printed collagen-Matrigel samples with Matrigel protein concentrations of 3 mg/ml, 4.5 mg/ml, or 6 mg/ml. All samples were 3D printed using a 254-μm-diameter nozzle at a printing speed of 40 mm/s. *$p \leq 0.05$; n.s., not significant.

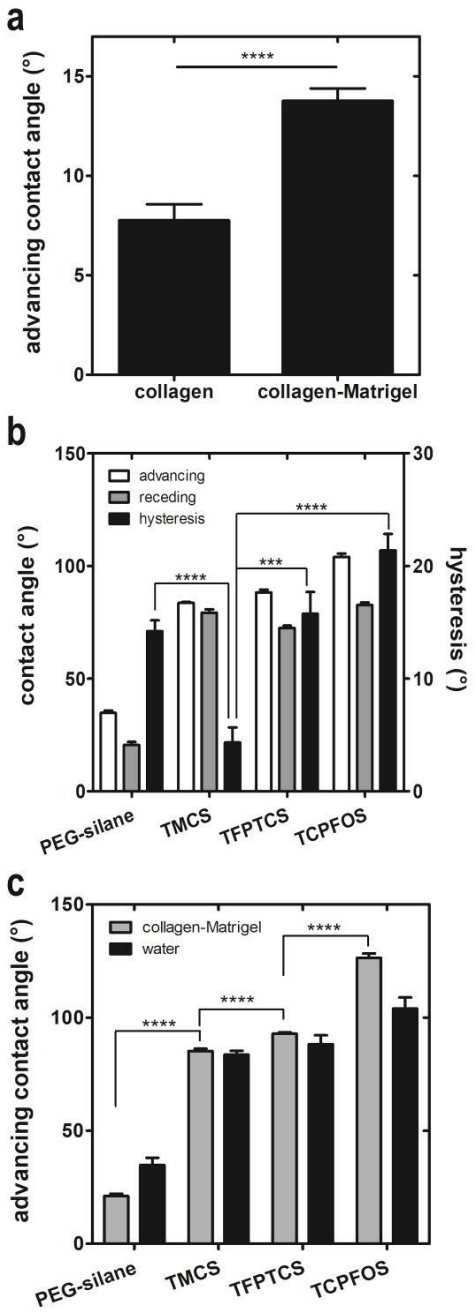

Figure S10. Contact angle measurements of collagen inks. a) Advancing contact angle measurements for collagen and collagen-Matrigel on untreated glass. b) Advancing and receding contact angles for water on silanized glass. c) Advancing contact angle measurements for collagen-Matrigel and water on silanized glass. The average of 10 experimental measurements is plotted for all contact angle data, and error bars represent standard error of the mean. Two-sided *p*-values were used for comparison. ***$p \leq 0.001$; ****$p \leq 0.0001$.

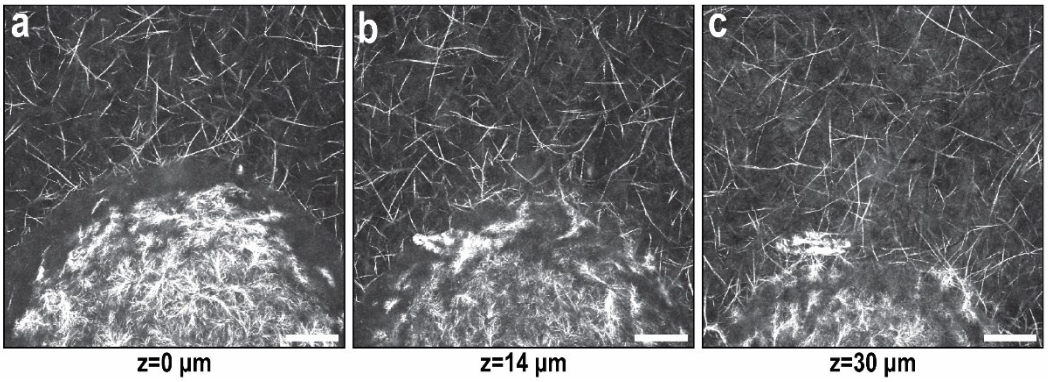

Figure S11. Collagen fiber alignment along a convex 3D-printed interface. CRM images of a convex interface between drop-cast collagen and 3D-printed collagen-Matrigel (Matrigel concentration = 5.8 mg/ml). Scale bars represent 100 µm. All CRM images represent a single confocal slice.

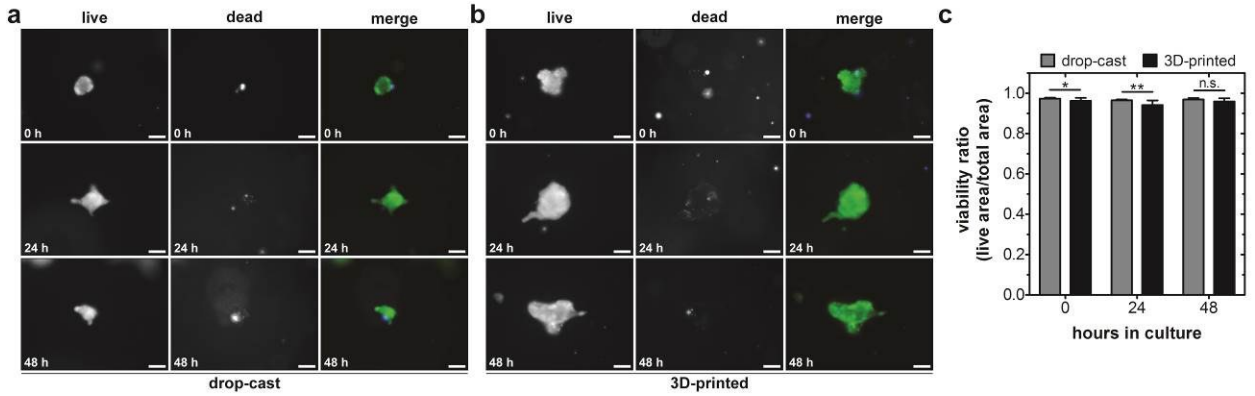

Figure S12. Live/dead staining of drop-cast and 3D-printed epithelial clusters. Representative fluorescence images of epithelial cell clusters after a) drop casting and b) 3D printing. c) Viability ratio, which represents the ratio of live cell area to total cell area. Epithelial clusters were stained with calcein AM to label live cells and ethidium homodimer-1 to label dead cells. In merged images, live cells are shown in green and dead cells are shown in blue. All images represent the maximum-intensity z-projection of a 20-μm z-stack. Scale bars represent 50 μm. The average of 9 replicates is plotted, and error bars represent standard deviation. *$p \leq 0.05$; **$p \leq 0.01$; n.s., not significant.